Cell Reports

Supplemental Information

Absence of SARM1 Rescues Development and Survival of NMNAT2-Deficient Axons

Jonathan Gilley, Giuseppe Orsomando, Isabel Nascimento-Ferreira, and Michael P. Coleman

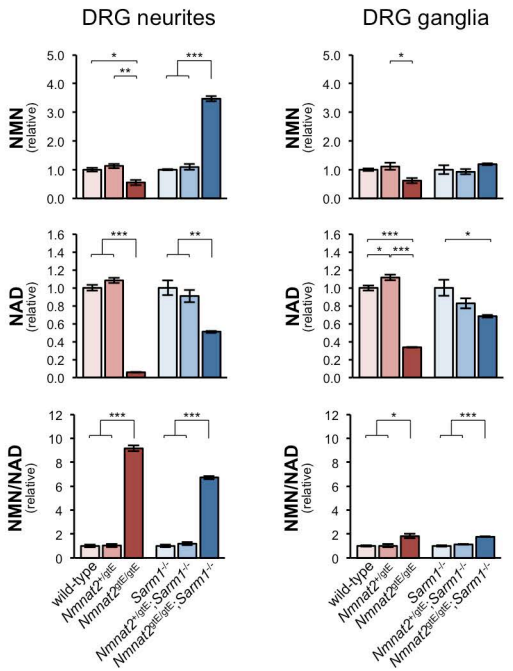

Figure S1. Changes in NMN and NAD resulting from a lack of NMNAT2 during development occur in the absence of SARM1, Related to Figure 3.

Relative changes in NMN, NAD and NMN/NAD ratio in DRG explant neurite and ganglia fractions from *Nmnat2* genotypes on either a wild-type *Sarm1* or *Sarm1*$^{-/-}$ background (n=3 for matched sets on each background prepared and assayed together). This confirms that the observed changes are very consistent and indicates that much of the variation in absolute NMN and NAD levels (Figure 3) can be attributed to session-to-session differences in culturing and processing.

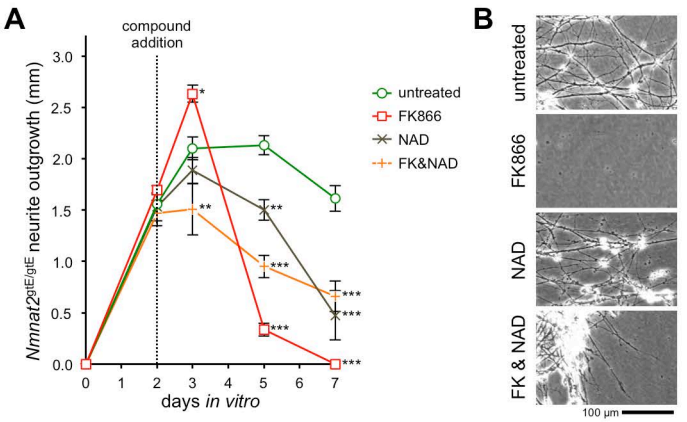

Figure S2. Rescued outgrowth of NMNAT2-deficient neurites by FK866 is not enhanced by NAD, Related to Figure 4.

(A) Quantification of neurite outgrowth over 7 days for explant cultures of DRGs taken from E18.5 *Nmnat2*$^{gtE/gtE}$ embryos treated with FK866 and/or NAD after 2 days *in vitro*. Means ±SEM are plotted (n=3-6 each treatment, statistical significance shown relative to untreated). (B) Representative phase contrast images showing the physical appearance of *Nmnat2*$^{gtE/gtE}$ DRG neurites (if present) at 5 days *in vitro* (3 days after the addition of the indicated compounds). Untreated and FK866 data and images in (A) and (B) are replicated from Figure 4C and 4D for comparison purposes.

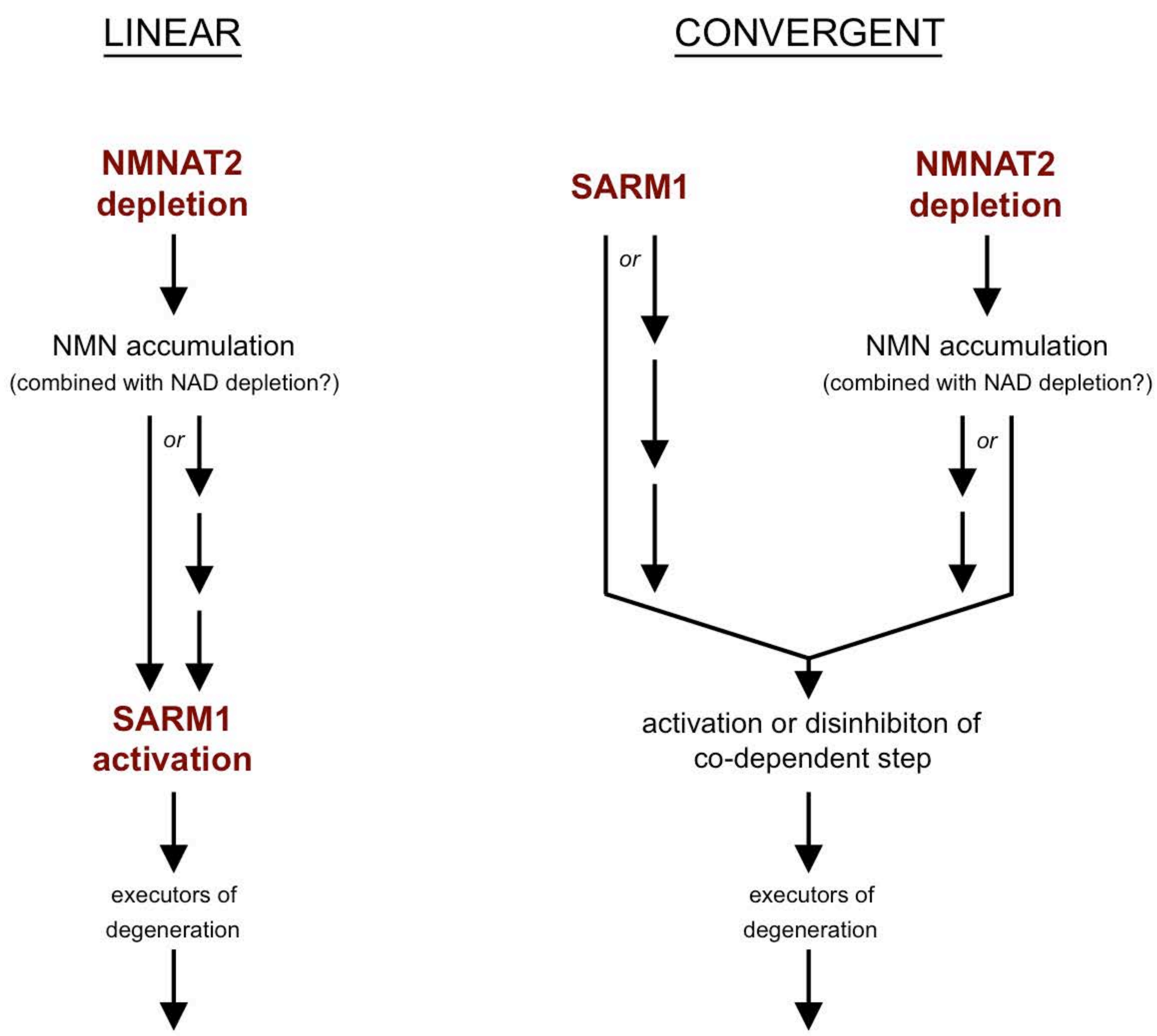

Figure S3. Alternative models of the relationship between NMNAT2 depletion and a SARM1 function in the WLD^S-sensitive axon degeneration pathway, Related to Figure 4.

Process pathways illustrating the possible relationships between NMNAT2 depletion, the resultant accumulation of NMN, and a pro-degenerative SARM1 function in the WLD^S-sensitive axon degeneration pathway. SARM1 could be activated by changes downstream of NMNAT2 loss in a linear pathway, either directly or via intermediate steps, or alternatively parallel SARM1-dependent and NMNAT2 loss-dependent branches of the pathway could converge at a co-dependent step upstream of the execution phase of degeneration.

SUPPLEMENTAL EXPERIMENTAL PROCEDURES

Primers for PCR genotyping and RT-PCR

Genotyping for the *Nmnat2*^{gtE} gene trap allele was performed as described previously (Gilley et al., 2013). *Sarm1* genotype was determined using two separate reactions. The first, using primers 5'-ACGCCTGGTTTCTTACTCTACG-3' and 5'-CCTTACCTCTTGCGGGTGATGC-3' amplifies a 508-bp product from the wild-type allele. The second, using primers 5'-GGTAGCCGGATCAAGCGTATGC-3' and 5'-CTCATCTCCGGGCCTTTCGACC-3' amplifies a 496-bp product from the neomycin resistance cassette retained in the knockout allele in place of deleted exons 3-6 (Kim et al., 2007). Primer annealing temperature was 60°C for both reactions.

The *Nmnat2* (exon 1-2) and *Actb* primers used for RT-PCR have been described previously (Gilley et al., 2013). *Sarm1* mRNA was detected using primers 5'-CTTCGCCAGCTACGCTACTTGC-3' and 5'-TTATCACGGGGTCCATCATCGT-3' (annealing at 60°C) that span exon 5-6. These exons are deleted in the knockout allele. Single, specific products were amplified using each primer set.

Antibodies used for immunoblotting

The following antibodies were used for immunoblotting; anti-NMNAT2 (Sigma, WH0023057M1) at 2 µg/ml, mouse monoclonal anti-SARM1 (Chen et al., 2011) at 1:5,000, anti-neuronal class βIII-Tubulin TUJ1 (Covance, MMS-435P) at 1:10,000, and mouse monoclonal anti-β-Actin (Sigma, A5316) at 1:5,000.

Constructs used in microinjections

A Dharmacon (Thermo Scientific) ON-TARGETplus SMART pool of siRNAs targeting murine *Nmnat2* (L-059190-01) and a non-targeting pool of siRNAs (D-001810-10) were used in this study. The SARM1-GFP expression vector consists of the entire

coding region of murine SARM1 cloned (by PCR) into pEFGP-N1 thereby placing the GFP tag at the C-terminus of the fusion protein. The GFP-NMN deamidase expression vector (pEGFP-C1-based) has been described previously (Di Stefano et al., 2014). Texas Red dextran, 10,000 MW, neutral (Life Technologies) was used in microinjection experiments in Figures 4A and 4B as it labels neurites rapidly allowing visualization of neurites prior to SARM1-GFP-induced degeneration which occurs within 24 hours. Expression of fluorescent proteins from injected plasmids was too slow for this purpose.

Image processing

Images were cropped using Adobe Photoshop Elements 11 and montages of overlapping fields of stained/labeled tissues were generated by pairwise stitching using an ImageJ plugin (Preibisch et al., 2009).

SUPPLEMENTAL REFERENCES

Chen, C.Y., Lin, C.W., Chang, C.Y., Jiang, S.T., and Hsueh, Y.P. (2011). Sarm1, a negative regulator of innate immunity, interacts with syndecan-2 and regulates neuronal morphology. J Cell Biol *193*, 769-784.

Preibisch, S., Saalfeld, S., and Tomancak, P. (2009). Globally optimal stitching of tiled 3D microscopic image acquisitions. Bioinformatics *25*, 1463-1465.